Microwave propagation in a magnetized inhomogeneous plasma slab using the Appleton–Hartree magnetoionic theory

M.S. Bawa'aneh, A.M. Al-Khateeb, and A.S. Sawalha

Abstract: Electromagnetic wave propagation in a nonuniform, collisional, magnetized plasma slab is investigated within magnetoionic theory. We allow for the presence of an ideal conductor at a distance d from the right transmissive plasma boundary, and derive the reflection, absorption, and transmission coefficients analytically for an arbitrary inhomogeneous plasma density profile. Dividing the inhomogeneous plasma slab into n thin layers allows for treating each layer as a homogeneous plasma and, therefore, the complex index of refraction of the magnetoionic theory is used to express the complex propagation vector of the waves in each layer. Upon matching the fields at all interfaces, a global matrix is formed that allows for the determination of the reflection, absorption, and transmission coefficients analytically. Results show that in the absence of the metallic wall, the reflected signal is a weak peak near ω_{ce}, while in the presence of the metallic wall this weak signal is overwhelmed by a strong transmitted peak from right to left after it has been reflected by the perfectly conducting metallic wall. Also, formation of a wider stealth band as the plasma density increases is observed.

PACS Nos: 52.25.Os, 52.40.Db, 42.50.Ct, 41.20.Jb

Résumé : Dans le cadre de la théorie magnéto-optique, nous étudions la propagation des ondes électromagnétiques dans une tranche de plasma non uniforme, collisionnel et magnétisé. Nous permettons la présence d'un conducteur idéal à une distance d à droite de la bordure du plasma transmissif et nous obtenons analytiquement les coefficients de réflexion, d'absorption et de transmission pour un plasma de profil de densité inhomogène et arbitraire. Diviser notre tranche inhomogène en n couches minces nous permet de traiter chaque couche comme un plasma homogène et par la suite, l'indice de réfraction complexe de la théorie magnéto-ionique est utilisé pour exprimer le vecteur complexe de propagation des ondes dans chaque couche. L'ajustement des champs à toutes les interfaces permet de former une matrice globale qui permet de déterminer analytiquement les coefficients de réflexion, d'absorption et de transmission. Les résultats indiquent qu'en l'absence d'un mur métallique, le signal réfléchi a un faible pic autour de ω_{ce}, alors qu'en présence d'un mur métallique, ce signal faible est complètement couvert par un fort pic de transmission de la droite vers la gauche, après qu'il sa réflexion par le mur parfaitement métallique. Nous observons aussi la formation de bandes furtives plus larges lorsque la densité du plasma augmente.

[Traduit par la Rédaction]

1. Introduction

Investigation of electromagnetic wave propagation in inhomogeneous magnetized plasma has, for years, attracted much attention due to its wide range of applications, particularly in telecommunication, where plasma may be used as an electromagnetic scatterer or absorber with potential applications to stealth technology. In most of the previous work, the nonuniform plasma is looked at as a series of plasma slabs, where the wave is partially absorbed in each slab and partially reflected and transmitted at each boundary between two consecutive slabs [1–7]. Butler et al. [2] have computed the phase and attenuation of millimetre waves in dielectric waveguides with thin surface plasma layers for various layer thicknesses. Laroussi and Roth [3] have studied numerically the effect of different plasma parameters on microwave propagation in nonuniform plasma of a series of subslabs. Hu et al. [4] have investigated the reflection, absorption, and transmission coefficients for a stratified plasma slab analytically for different plasma parameters using the scattering matrix method. Petrin [5] has investigated the possible transmission of microwaves through a plasma layer with electron concentration more than the critical value and applied his parametric investigation to the transparency conditions of the shock wave plasma. Also, reflection characteristics of electromagnetic waves from multilayer magnetized plasma was studied by Tang et al. [6] and those for nonmagnetized plasma by Ma et al. [7]. Recently, Yuan et al. [8] considered electromagnetic wave absorption on a structure of nonmagnetized plasma and a radar-absorbing material near a perfect conduc-

M.S. Bawa'aneh. Khalifa University of Science Technology and Research, P.O. Box 573, Sharjah, United Arab Emirates; The Hashemite University, P.O. Box 150459, Zarqa, Jordan.
A.M. Al-Khateeb and A.S. Sawalha. King Faisal University, P.O. Box 400, Al-Hufof, Kingdom of Saudi Arabia.

Corresponding author: M.S. Bawa'aneh (e-mail: m.bawaaneh@kustar.ac.ae).

tor. They found that the electromagnetic wave attenuation is strongly affected by the plasma parameters as well as the radar-absorbing material parameters.

The present work is concerned with the analytical derivation and numerical investigation of expressions for the reflection, absorption, and transmission coefficients of electromagnetic waves in a nonuniform, collisional, magnetized plasma slab by making use of the complex index of refraction of the magnetoionic theory of a cold, homogeneous, collisional, magnetized plasma [4, 9–11]. Because of the inhomogeneity of the plasma slab under consideration, the plasma refractive index $\sqrt{\varepsilon(\omega)}$ will generally vary with the plasma density profile, where $\varepsilon(\omega)$ is the plasma longitudinal dielectric function. By dividing the plasma slab into N uniform layers, each layer will have its own magnetoionic index of refraction (or wave propagation constant) and will be treated as a uniform plasma.

The overall effect of the inhomogeneity of the plasma slab will be accounted for by matching the fields at the interfaces between the adjacent layers. At each interface between any two adjacent layers of the plasma slab, say m and $m + 1$, there will be two different values for the permittivity $\varepsilon^{(m)} = \varepsilon_0 \varepsilon^{(m)}(\omega)$ and $\varepsilon^{(m+1)} = \varepsilon_0 \varepsilon^{(m+1)}(\omega)$, and two different wave propagation constants, $k^{(m)} = \omega/c \sqrt{\varepsilon^{(m)}(\omega)}$ and $k^{(m+1)} = \omega/c \sqrt{\varepsilon^{(m+1)}(\omega)}$, where ε_0 is the permittivity of free space, ω is the wave frequency, and c the speed of light in vacuum. Further, we allow for the presence of an ideal conductor a distance d from the right transmissive plasma boundary, which in turn leads to the formation of standing wave patterns in the region to the right of the transmissive plasma boundary. In the presence of the conducting wall, possible modifications on the total reflection and transmission coefficients will be investigated in this work.

The paper is organized as follows. In Sect. 2, the model equations are presented and the reflection, absorption, and transmission coefficients are derived and compared with those found in the literature. Numerical results are presented in Sect. 3. Comments and conclusions are presented in Sect. 4.

2. Problem formulation

We consider a linearly polarized plane wave such that $E(x, t) = E_z(x, t)\hat{z}$. The wave is incident on a magnetized, collisional, and inhomogeneous plasma slab extending from $x = 0$ to $x = a$. For $x < 0$ the surrounding region of incidence has a permittivity $\varepsilon^{(L)} = \varepsilon_0 \varepsilon^{(L)}(\omega)$, while it is $\varepsilon^{(R)} = \varepsilon_0 \varepsilon^{(R)}(\omega)$ in the medium to the right of the plasma slab interface at $x = a$. The transmissive region for $a < x < b$ has a width $d = b - a$ and supports the formation of standing wave patterns due to the presence of an ideal conductor at $x = b$. The plasma slab is divided into n homogeneous layers with $d_{m+1} - d_m$ being the width of the mth layer, where $m = 1, 2, 3, \ldots, n$. The incident, reflected, and transmitted waves propagate along x, perpendicular to the background uniform magnetic field in the y-direction, such that $\boldsymbol{B} = B_0\hat{y}$, as shown in Fig. 1. In the region of incidence to the left of the plasma slab, the total time-harmonic electric field is given by

$$E_z^{(L)}(x, t) = E_0 \, e_z^{(L)}(x)\mathrm{e}^{i\omega t} \tag{1}$$

Fig. 1. Geometry of the problem.
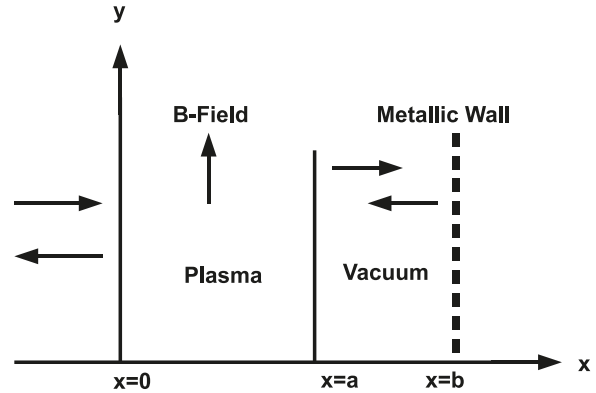
$$e_z^{(L)}(x) = \exp\left(-ik_x^{(L)}x\right) + A \exp\left(ik_x^{(L)}x\right) \tag{2}$$

where E_0 is the amplitude of the incident field, A the global reflection coefficient of the region of incidence, and $k_x^{(L)}$ is the wave propagation constant in the region of incidence such that $k^{(L)} = \omega/c\sqrt{\varepsilon^{(L)}(\omega)}$. Following the magnetoionic theory [12], the variation of the wave propagation constant is ignored over the homogeneous mth plasma layer, and therefore, the total wave in the mth layer can be written as follows:

$$E_z^{(m)}(x, t) = E_0 \, e_z^{(m)}(x)\mathrm{e}^{i\omega t} \tag{3}$$

$$e_z^{(m)}(x) = B_m \exp\left(-ik_x^{(m)}x\right) + C_m \exp\left(ik_x^{(m)}x\right) \tag{4}$$

where B_m and C_m are the partial transmission and reflection coefficients, respectively. The total wave in the transmissive region between $x = a$ and $x = b$ is

$$E_z^{(R)}(x, t) = E_0 \, e_z^{(R)}(x)\mathrm{e}^{i\omega t} \tag{5}$$

$$e_z^{(R)}(x) = D \exp\left(-ik_z^{(R)}x\right) + F \exp\left(ik_z^{(R)}x\right) \tag{6}$$

Here, D stands for the global transmission coefficient and F is the global reflection coefficient of the region of transmission. The relation between D and F is established by the vanishing of $E_z^{(R)}(x, t)$ at $x = b$. Accordingly, the electric field, $e_z^{(R)}(x)$, of (6) takes on the following form:

$$e_z^{(R)}(x) = -2iD \exp\left(-ik_x^{(R)}b\right) \sin k_x^{(R)}(x - b) \tag{7}$$

$$F = -D \exp\left(-2ik_x^{(R)}b\right) \tag{8}$$

where propagation constant $k^{(R)}$ in the region to the right of the plasma slab is $k^{(R)} = \omega/c\sqrt{\varepsilon^{(R)}(\omega)}$. The unknown coefficients A, B_m, C_m, and D will be determined by matching the tangential electric field, E_z, and the tangential magnetic field, $H_y = -(i/\mu_0\omega)\partial E_z/\partial x$, at all interfaces involved, namely, at $x = 0$, $x = a$, and at all interfaces between adjacent layers within the plasma slab.

The continuity of the tangential electric field, E_z, and magnetic field, H_y, at the interface between the incidence region and the first plasma layer, yield the following two equations presented in matrix form

$$\begin{bmatrix} B_1 \\ C_1 \end{bmatrix} = \mathbf{S}_1 \begin{bmatrix} A \\ 1 \end{bmatrix} \tag{9}$$

where $\mathbf{S}_1$ is given by

$$\mathbf{S}_1 = \begin{bmatrix} 1 & 1 \\ k_x^{(1)} & -k_x^{(1)} \end{bmatrix}^{-1} \begin{bmatrix} 1 & 1 \\ k_x^{(0)} & -k_x^{(0)} \end{bmatrix}$$
$$= \frac{1}{2k_x^{(1)}} \begin{bmatrix} k_x^{(1)} & -k_x^{(L)} & k_x^{(1)} & +k_x^{(L)} \\ k_x^{(1)} & +k_x^{(L)} & k_x^{(1)} & -k_x^{(L)} \end{bmatrix} \tag{10}$$

The same matching conditions applied on the boundary between any two consecutive layers, say the m and $m - 1$ layers, yield the following system of equations:

$$\begin{pmatrix} B_m \\ C_m \end{pmatrix} = \mathbf{S}_m \begin{pmatrix} B_{m-1} \\ C_{m-1} \end{pmatrix} \tag{11}$$

where m in (11) varies from $m = 2$ to $m = n$, matrix $\mathbf{S}_m$ is given by

$$\mathbf{S}_m = \begin{bmatrix} \exp\left(-ik_x^{(m)}d_m\right) & \exp\left(ik_x^{(m)}d_m\right) \\ k_x^{(m)}\exp\left(-ik_x^{(m)}d_m\right) & -k_x^{(m)}\exp\left(ik_x^{(m)}d_m\right) \end{bmatrix}$$
$$\times \begin{bmatrix} \exp\left(-ik_x^{(m-1)}d_m\right) & \exp\left(ik_x^{(m-1)}d_m\right) \\ k_x^{(m-1)}\exp\left(-ik_x^{(m-1)}d_m\right) & -k_x^{(m-1)}\exp\left(ik_x^{(m-1)}d_m\right) \end{bmatrix}$$
$$\equiv \frac{1}{2k_x^{(m)}} \begin{bmatrix} \alpha_{11} & \alpha_{12} \\ \alpha_{21} & \alpha_{22} \end{bmatrix} \tag{12}$$

and the elements of matrix $\mathbf{S}_m$ are given by

$$\alpha_{11} = \left[k^{(m)} + k^{(m-1)}\right] \exp\left[id_m\left(k^{(m)} - k^{(m-1)}\right)\right]$$

$$\alpha_{12} = \left[k^{(m)} - k^{(m-1)}\right] \exp\left[id_m\left(k^{(m)} + k^{(m-1)}\right)\right]$$

$$\alpha_{21} = \left[k^{(m)} - k^{(m-1)}\right] \exp\left[-id_m\left(k^{(m)} - k^{(m-1)}\right)\right]$$

$$\alpha_{22} = \left[k^{(m)} + k^{(m-1)}\right] \exp\left[-id_m\left(k^{(m)} - k^{(m-1)}\right)\right]$$

The tangential fields are now matched at $x = a$. From the continuity of E_z and H_y at $x = a$, we obtain the following system of equations:

$$\begin{bmatrix} B_n \\ C_n \end{bmatrix} = D\mathbf{V} \tag{13}$$

where the column vector $\mathbf{V}$ is given by

$$\mathbf{V} = \begin{bmatrix} \exp\left(-ik_x^{(n)}a\right) & \exp\left(ik_x^{(n)}a\right) \\ k_x^{(n)}\exp\left(-ik_x^{(n)}a\right) & -k_x^{(n)}\exp\left(ik_x^{(n)}a\right) \end{bmatrix}^{-1}$$
$$\times 2\exp\left(-ik_x^{(R)}b\right) \begin{bmatrix} i\sin\left(k_x^{(R)}d\right) \\ k_x^{(R)}\cos\left(k_x^{(R)}d\right) \end{bmatrix}$$

which, when simplified, gives

$$\mathbf{V} = \begin{bmatrix} v_1 \\ v_2 \end{bmatrix} \tag{14}$$

with the elements of the $\mathbf{V}$ column vector, namely v_1 and v_2, given by

$$v_1 = \frac{\exp\left(ik_x^{(n)}a - ik_x^{(R)}b\right)}{k_x^{(n)}}$$
$$\times \left[ik_x^{(n)}\sin\left(k_x^{(R)}d\right) + k_x^{(R)}\cos\left(k_x^{(R)}d\right)\right]$$

$$v_2 = \frac{\exp\left(-ik_x^{(n)}a - ik_x^{(R)}b\right)}{k_x^{(n)}}$$
$$\times \left[ik_x^{(n)}\sin\left(k_x^{(R)}d\right) - k_x^{(R)}\cos\left(k_x^{(R)}d\right)\right]$$

Combining (9), (11), and (13) to eleminate the local coefficients B and C yields the following sytem for the coefficients A and D:

$$\mathbf{S} \begin{bmatrix} A \\ 1 \end{bmatrix} = D\mathbf{V} \tag{15}$$

where the matrix $\mathbf{S}$ is directly obtained from (11) by assuming $m \to m - 1$ and iterating the process n times (n being the number of sublayers). The resulting formula for matrix $\mathbf{S}$ is

$$\mathbf{S} = \left(\prod_{m=n}^{2} \mathbf{S}_m\right) \mathbf{S}_1 \tag{16}$$

Upon writing the resulting product matrix of (16) in the form

$$\mathbf{S} = \begin{bmatrix} a_{11} & a_{12} \\ a_{21} & a_{22} \end{bmatrix} \tag{17}$$

we arrive at the following closed form for the two coefficients A and D:

$$\begin{bmatrix} A \\ D \end{bmatrix} = \frac{1}{a_{11}v_2 - a_{21}v_1} \begin{bmatrix} -v_2 & v_1 \\ -a_{12} & a_{11} \end{bmatrix} \begin{bmatrix} a_{12} \\ a_{22} \end{bmatrix} \tag{18}$$

Equation (18) gives, in closed form, the normalized global reflection and transmission coefficients for an electromagnetic wave incident on plasma.

3. Numerical results

In this section, we present numerical examples of the effect of plasma parameters on reflection, absorption, and transmission of electromagnetic waves in nonuniform magnetized plasma. We consider an exponentially increasing plasma density profile such that $N = N_0 e^{\alpha x}$, where N_0 is the plasma density at the incidence interface $x = 0$ and α is a positive constant, and we divide the plasma slab into n layers with the plasma density being N_m within the mth layer.

The magnetoionic Appleton–Hartree theory was developed to describe electromagnetic wave propagation in ionized media in the presence of static magnetic fields (see e.g., ref. 12). Magnetoionic and optical-ray theories lead to useful and satisfactory description of wave propagation and reflection.

Within the magnetoionic theory combined with the optical ray theory, waves are assumed to be of a plane wave nature with a complex propagation constant, namely, they vary as $e^{i\omega t - Kx}$ with all the dynamical effects being included in the complex propagation constant K.

In the presence of a perpendicular background magnetic field the plasma in general is anisotropic, and it sustains two modes; an ordinary mode along the B-field and an extraordinary mode perpendicular to the B-field. By the Appleton–Hartree theory, the dynamical effect is reduced into a modification in the longitudinal plasma dielectric function. Within each layer of the plasma slab, the longitudinal plasma dielectric function $\varepsilon^{(m)}$ of the mth layer for perpendicular wave propagation at frequency ω used in all numerical examples is given by [9, 10, 12]

$$\varepsilon^{(m)}(\omega) = -1$$
$$- \left\{ F - \frac{D_T^2}{2(1+F)} \pm \sqrt{\frac{D_T^4}{4(1+F)^2} + D_L^2} \right\}^{-1} \quad (19)$$

$$F = A + iB \qquad A = -\frac{\omega^2}{\omega_{p,m}^2} \qquad B = \frac{\omega v}{\omega_{p,m}^2} \quad (20)$$

$$D_T = \frac{\omega \mu \varepsilon H_T}{n_e e} \qquad D_L = \frac{\omega \mu \varepsilon H_L}{n_e e} \quad (21)$$

where $\omega_{p,m}$ is the mth layer plasma frequency, ω_{ce} the electron gyro-frequency, v the effective collision frequency (which accounts for losses in the plasma slab), e the elementary charge, and n_e is the electron plasma density. Here H_L and H_T are, respectively, the magnetic field components along and normal to the direction of wave propagation.

Equation (19) known as the magnetoionic equation was first derived by Appleton and independently by Hartree. The plus and minus signs in (19) show that the medium supports two characteristic modes. Also, the propagation constant, K, can take two values and, therefore, an incident wave will split into two wave components with different phase velocities, polarizations, and absorptions. These waves are usually assigned as ordinary and extraordinary waves. For propagation normal to a magnetic field, the plus sign represents an ordinary mode and the minus sign represents the extraordinary mode. In our numerical analysis, (19) for the propagation and absorption of the extraordinary mode is used for the case $H_L = 0$.

Figure 2 shows the absorption versus wave frequency with (solid line) and without (dotted line) the conducting wall at $x = b$. Other parameters used to produce the figure are cyclotron frequency $f_{ce} = \omega_{ce}/2\pi = 4$ GHz, collision frequency $f_{col} = v/2\pi = 0.02 f_{ce}$, $N_0 = 10^{15}$ m^{-3}, $a = 10$ cm, and $d = 5$ cm. Both curves show peak absorption values at wave frequencies in the vicinity of electron cyclotron frequency, $\omega \approx \omega_{ce}$. The absorption is higher in the presence of the metallic wall as waves travel more in the plasma (incident wave traveling from left to right and wave reflected from the metallic wall reenters the plasma and travels from right to left). Figure 3 explains the difference in the morphology of the reflected intensity in the two cases with (Fig. 3a) and without (Fig. 3b) the metallic wall. The curves of Fig. 3 show that in

Fig. 2. Normalized absorbed intensity versus wave frequency (GHz) for plasma with (solid line) and without (dotted line) a reflecting conductor. Parameters are $f_{ce} = 4$ GHz, $v = 0.02\ \omega_{ce}$, $N_0 = 10^{15}$ m^{-3}, $a = 10$ cm, and $d = 5$ cm.
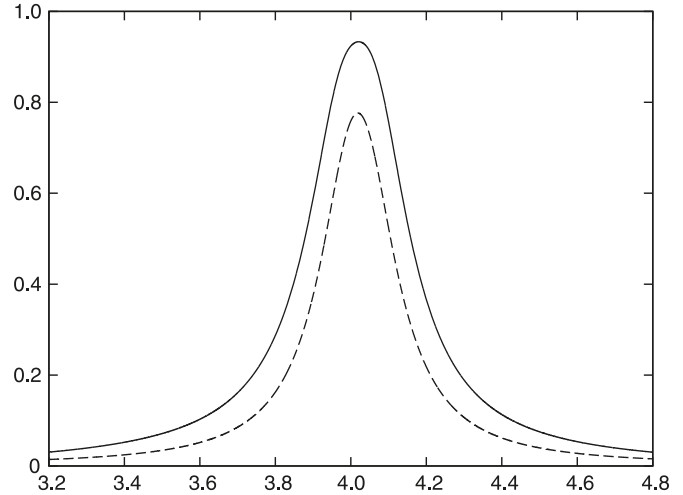
the absence of the metallic wall the reflected signal is a weak peak near ω_{ce} (see e.g., ref. 4), while this weak signal is overwhelmed by strong transmission from right to left after the wave has been reflected by the perfectly conducting metallic wall.

Figure 4 shows absorption versus wave frequency for four different initial plasma densities N_0. Other parameters are $f_{ce} = 3$ GHz, $v = 0.1\ \omega_{ce}$, $a = 30$ cm, and $d = 5$ cm. Narrow to wide peaks correspond to $N_0 = 10^{15}$, 10^{16}, 10^{17}, and 5×10^{17}. Here we observe the formation of a wider stealth band as the plasma thickness increases. Controlling the plasma parameters and the thickness of the gap between the plasma slab and the conducting wall, one can control the range of almost full absorption; For example, for $N_0 = 10^{17}$, $f_{ce} = 3$ GHz, $v = 0.1\ \omega_{ce}$, $a = 30$ cm, and $d = 5$ cm, one can obtain almost a full absorption of the C-band. This result is in qualitative agreement with that in ref. 8. Yuan et al., however, deal with nonmagnetized plasma and miss the broad absorption peak resonant with the electron cyclotron frequency.

Figures 5 and 6 show absorption and reflection, respectively, versus the wave frequency 2 MHz $< f <$ 6 MHz and width 0 cm $< a <$ 25 cm of the plasma slab. Inner to outer contours in Fig. 5 correspond to absorption values 0.8, 0.6, 0.4, and 0.2. In Fig. 6, inner to outer contours correspond to absorption values 0.2, 0.4, 0.6, and 0.8. We observe that as the plasma thickness increases, both absorption and reflection peaks in the ω_{ce} vicinity widen and strengthen.

Figures 7 and 8 show absorption and reflection, respectively, versus wave frequency 1 MHz $< f <$ 5 MHz and effective collision frequency 0 MHz $< f_{col} <$ 0.3 MHz. Inner to outer contours in Fig. 7 correspond to absorption values 0.8, 0.6, 0.4, and 0.2, while those of Fig. 8 correspond to 0.2, 0.4, 0.6, and 0.8. Results show a weak increase in absorption as the collision frequency increases. This is due to the increase in absorption of energy from the wave as a result of more momentum transfer from electrons to neutral particles as collision frequency increases.

Fig. 3. Normalized reflected intensity versus wave frequency (GHz) for plasma (*a*) with and (*b*) without a reflecting conductor. Parameters are $f_{ce} = 4$ GHz, $\nu = 0.02\ \omega_{ce}$, $N_0 = 10^{15}$ m^{-3}, $a = 10$ cm, and $d = 5$ cm.
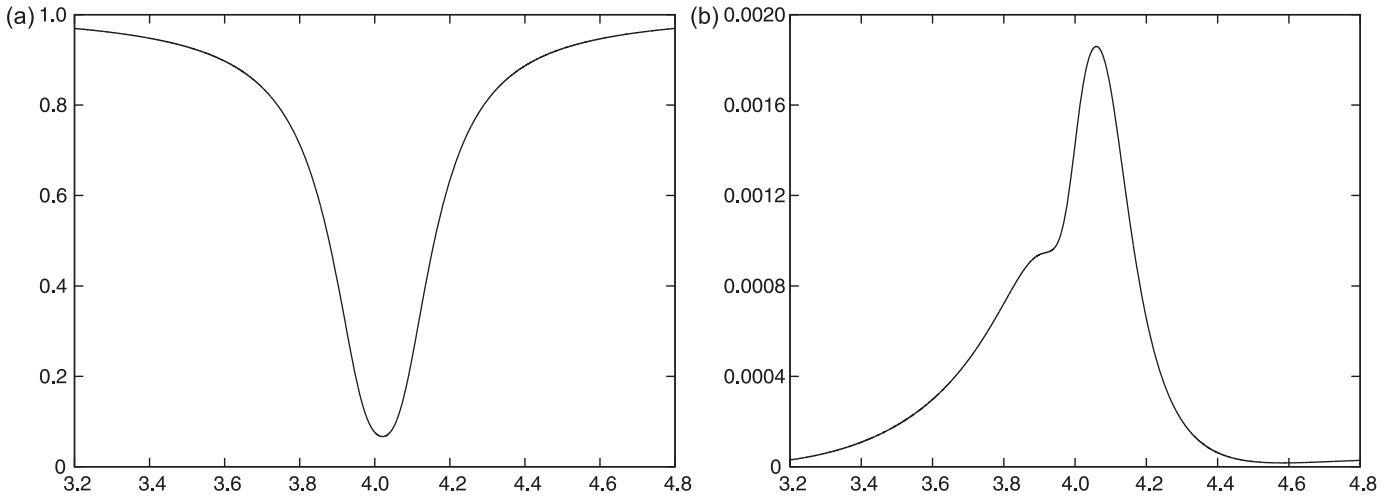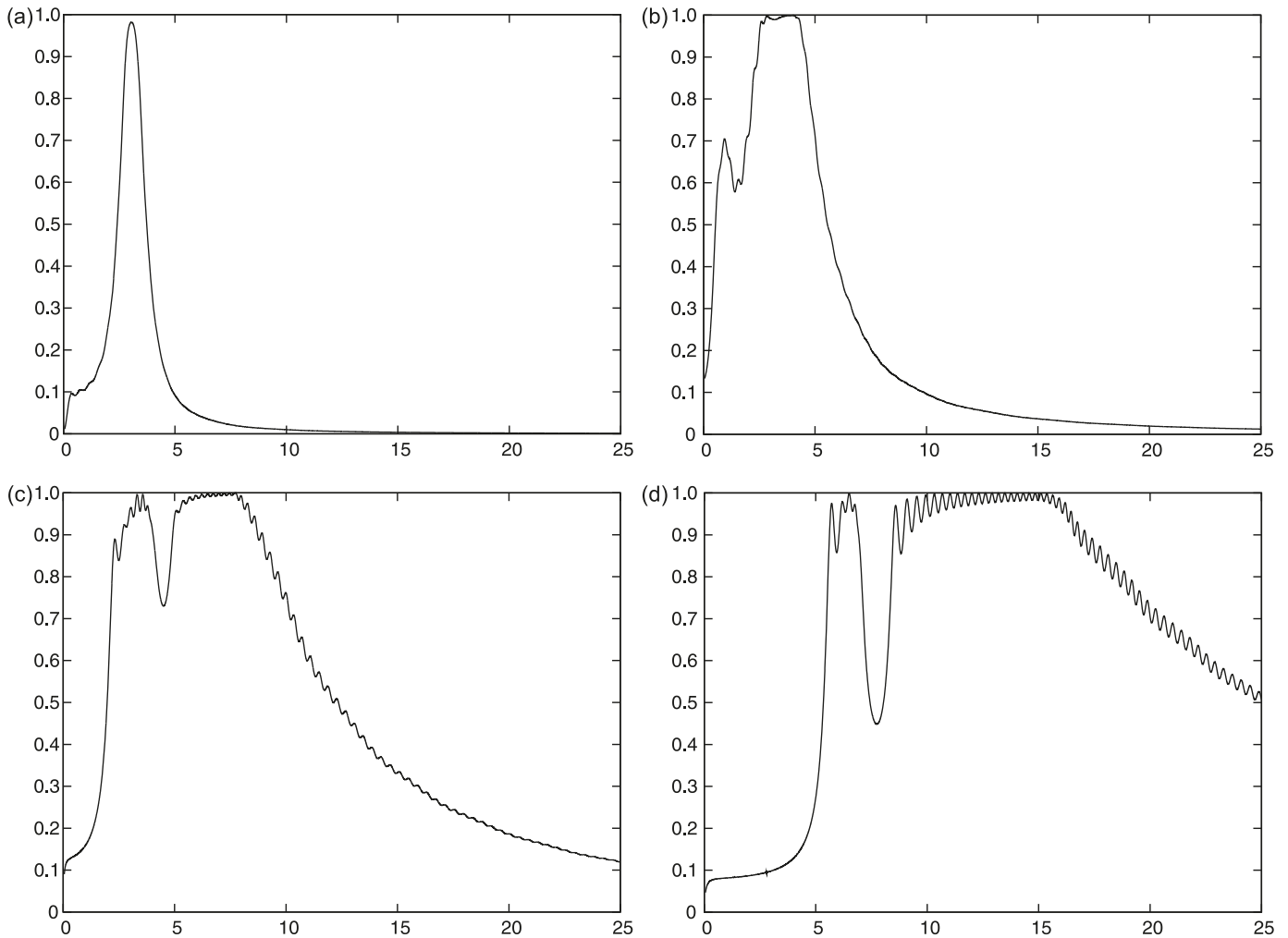

Fig. 4. Normalized absorbed intensity versus wave frequency (GHz) for plasma with a reflecting conductor for different values of plasma density: $N_0 = $ (*a*) 10^{15}, (*b*) 10^{16}, (*c*) 10^{17}, and (*d*) 5×10^{17}. Other parameters are $f_{ce} = 3$ GHz, $\nu = 0.1\ \omega_{ce}$, $a = 30$ cm, and $d = 5$ cm.

4. Comments and conclusion

The paper presents analytical derivation and numerical investigation of the reflection, absorption, and transmission coefficients of extraordinary electromagnetic waves in a cold, nonuniform, collisional, magnetized plasma slab using Appleton–Hartree magnetoionic theory. The presence of an

Fig. 5. Normalized absorbed intensity versus wave frequency (GHz) and plasma thickness (cm) for plasma with a reflecting conductor. Parameters are $f_{ce} = 4$ GHz, $\nu = 0.1\ \omega_{ce}$, $N_0 = 10^{15}$ m^{-3}, and $d = 5$ cm.
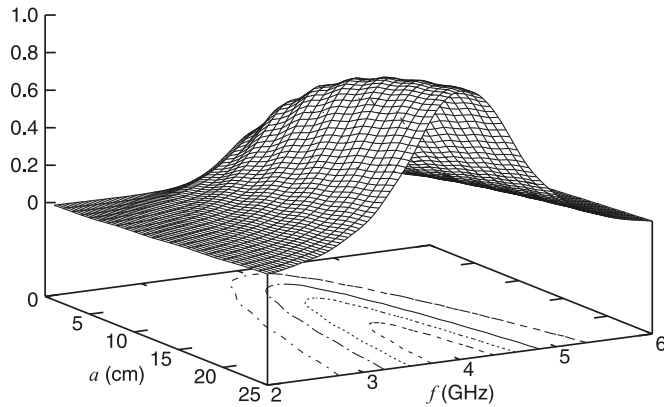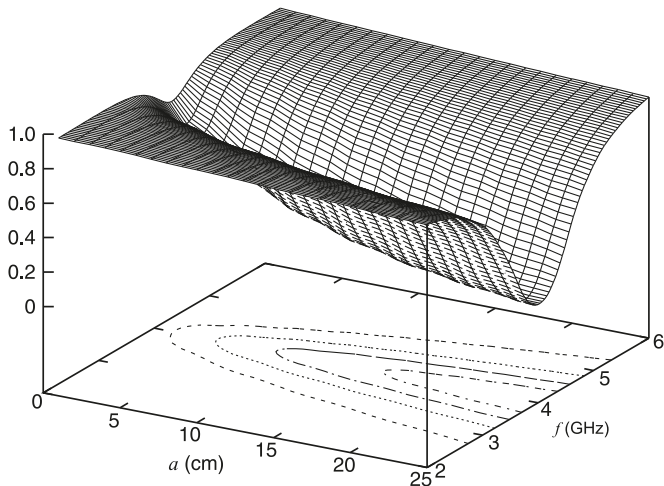
Fig. 6. Normalized reflected intensity versus wave frequency (GHz) and plasma thickness (cm) for plasma with a reflecting conductor. Parameters are $f_{ce} = 4$ GHz, $\nu = 0.1\ \omega_{ce}$, $N_0 = 10^{15}$ m^{-3}, and $d = 5$ cm.

Fig. 7. Normalized absorbed intensity versus wave and collision frequencies (GHz). Parameters are $f_{ce} = 4$ GHz, $N_0 = 10^{15}$ m^{-3}, $a = 30$ cm, and $d = 5$ cm.

Fig. 8. Normalized reflected intensity versus wave and collision frequencies (GHz). Parameters are $f_{ce} = 4$ GHz, $N_0 = 10^{15}$ m^{-3}, $a = 30$ cm, and $d = 5$ cm.
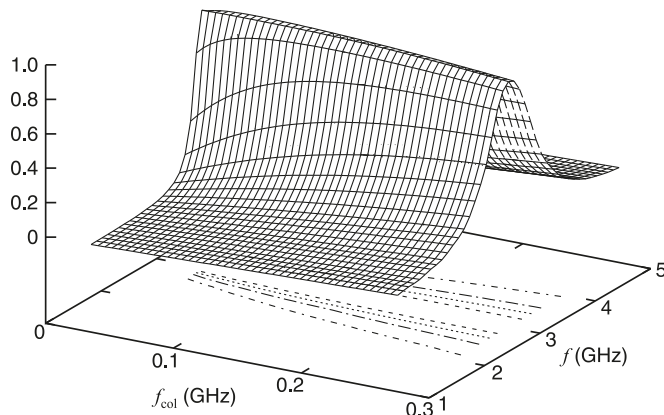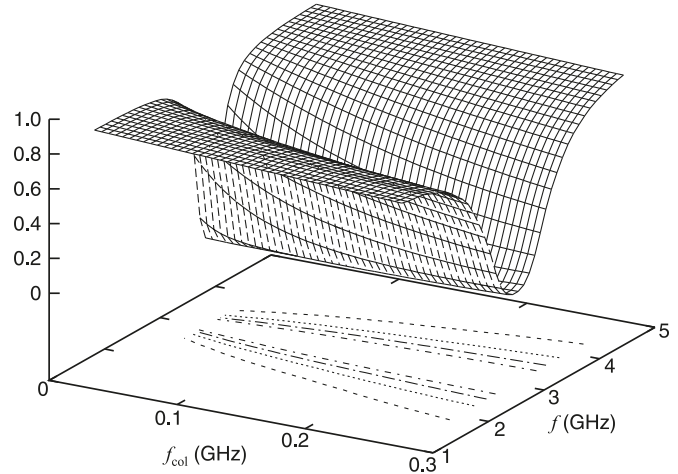
ideal conducting surface at a distance d from the right transmissive plasma boundary allows for the formation of standing waves. Modifications on the local and global scattering matrices and on the total reflection and transmission coefficients have been investigated numerically in a series of figures for different parameters. In the absence of the metallic wall, the reflected signal is a weak peak near ω_{ce}, while in the presence of the metallic wall this weak signal is overwhelmed by a strong transmitted peak from right to left after it has been reflected by the perfectly conducting metallic wall. Results show the formation of a wider stealth band as the plasma thickness increases, and a weak increase in absorption as the collision frequency increases. As mentioned earlier, for $N_0 = 10^{17}$, $f_{ce} = 3$ GHz, $\nu = 0.1\ \omega_{ce}$, $a = 30$ cm, and $d = 5$ cm, one can obtain almost a full absorption of the C-band.

In a collisionless cold plasma, waves are reflected at the bulk plasma frequency ω_p. There is a stopband for wave propagation for frequencies below ω_p, and the passband exists for $\omega > \omega_p$ [13, 14]. In the presence of collisions, the propagation characteristics are altered considerably if the collision frequency ν approaches or superpasses the plasma frequency. Higher collision frequencies can lead to weaker absorption. Waves are then allowed to propagate in plasmas at frequencies below ω_p and the stopband becomes narrower as ν increases and disappears at $\omega_p \approx \nu$. For $\nu > \omega_p$ there will be no stopband, and waves will propagate, although attenuated, at all frequencies [13, 15].

Within the Appleton–Hartree theory, motion of plasma ions is not important, and the plasma ions are treated as a neutralizing background of positive charges. In the simplified treatment of a plasma as a dielectric medium, convection currents resulting from the plasma electrons and ions are accounted for in the derivation of the equivalent dielectric permittivity ε [13, 15, 16]. It is well known that electromagnetic waves cannot propagate in an overdense plasma if the plasma frequency is above the excitation frequency. Waves are reflected at the bulk plasma frequency and become evanescent waves [14, 17, 18]. This may give rise to heating of the plasma and then waves do not travel any more in the radial direction, but rather propagate along the plasma–vacuum

or plasma–metal interfaces. The wave energy is then transferred to the plasma by the evanescent wave, which enters the plasma perpendicular to its surface and decays exponentially.

References

1. G.H. Price. Radio Sci. J. Res. **68D**, 407 (1964).
2. J.K. Butler, T.-F. Wu, and M.W. Scott. IEEE Trans. Microw. Theory Tech. **34**, 147 (1986). doi:10.1109/TMTT.1986. 1133292.
3. M. Laroussi and J.R. Roth. IEEE Trans. Plasma Sci. **21**, 366 (1993). doi:10.1109/27.234562.
4. B.J. Hu, G. Wei, and S.L. Lai. IEEE Trans. Plasma Sci. **27**, 1131 (1999). doi:10.1109/27.782293.
5. A.B. Petrin. IEEE Trans. Plasma Sci. **28**, 1000 (2000). doi:10. 1109/27.887768.
6. D.L. Tang, A.P. Sun, X.M. Qiu, and P.K. Chu. IEEE Trans. Plasma Sci. **31**, 405 (2003). doi:10.1109/TPS.2003.811648.
7. L.X. Ma, H. Zhang, and C.X. Zhang. J. Electromagn. Waves Appl. **22**, 2285 (2008). doi:10.1163/156939308787543877.
8. C.-X. Yuan, Z.-X. Zhou, J.W. Zhang, X.-L. Xiang, Y. Feng, and H.-G. Sun. IEEE Trans. Plasma Sci. **39**, 1768 (2011). doi:10.1109/TPS.2011.2160285.
9. E.V. Appleton. J. Inst. Elec. Eng. **71**, 642 (1932).
10. D.R. Hartree. Proc. Camb. Philos. Soc. **25**, 97 (1929). doi:10. 1017/S0305004100018600.
11. J. Zhang and Z. Liu. Int. J. Infrared Millim. Waves, **28**, 71 (2007). doi:10.1007/s10762-006-9176-6.
12. R.S. Macmillan. Some properties of the ionosphere at low radio frequencies, Ph.D. thesis, California Institute of Technology, Pasadena, Calif. 1954. Chap. III, pp. 12–24.
13. C.C. Johnson. Field and wave electrodynamics. McGraw-Hill, New York. 1965. p. 403.
14. A.W. Trivelpiece and R.W. Gould. J. Appl. Phys. **30**, 1784 (1959). doi:10.1063/1.1735056.
15. N.A. Kral and A.W. Trivelpiece. Principles of plasma physics. McGraw-Hill, New York. 1973.
16. I.P. Shkarofsky, T.W. Johanson, and P.M. Bachynski. The particle kinetics of plasmas. Addision-Wesley, Reading. 1966.
17. A.D. Boardman. Electromagnetic surface modes. Wiley, New York. 1982.
18. Y.M. Aliev, H. Schlüter, and A. Shivarova. Guided-wave-produced plasmas. Springer, Berlin. 2000. p. 31.